amplifier, on the rising edge of the clock signal. This improves the reliability of operation and latching speed.

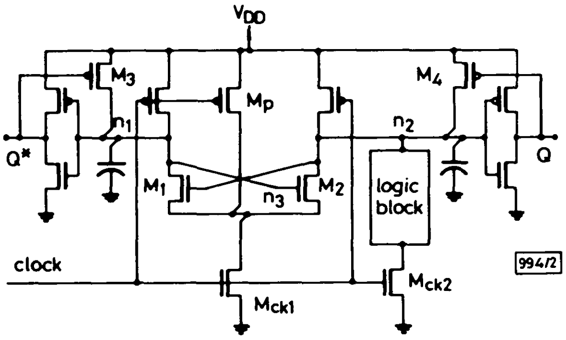

Fig. 2 *Improved ldomino gate*

The latched domino (ldomino) technique proposed here is capable of generating both an inverting and noninverting domino output signal from a gate of arbitrary complexity. However, this technique can only be applied to the first stage of logic in a series of domino gates, if the glitch-free property of domino logic is to be preserved. Ldomino gates can therefore drive domino gates, but cannot be driven directly by domino gates, since glitch-free operation requires that the inputs to the gate should stabilise during the precharge clock phase. This limitation is not as serious as it sounds, since any logic function can be performed in two stages (cf. a PLA). The fact that inverting gates are possible in the first stage of domino logic offers a significant improvement in logic flexibility over standard domino. The other significant advantage of the ldomino technique over standard domino, is the substantial reduction in wiring overhead. This is the result of the fact that the ldomino technique is capable of generating a logic function, as well as its complement, without requiring that input signals be complemented, which in the worst case can double the area required by the interconnect. This area advantage is equally significant when compared to DCVSL,[2] which requires fully differential inputs as well as outputs. Ldomino uses single-ended inputs to the logic block and uses inverted variables only where actually required by the logic function implemented.

Since the ldomino technique belongs to the domino family, it retains the speed advantage of domino logic. Ldomino circuits are fully compatible with, and can be combined with, standard domino and DCVSL in the same circuit, in order to make optimal use of all three alternatives.

The circuit illustrated in Fig. 1 was implemented in a 5 μm silicon gate CMOS process. Measurements on the gates indicated a typical delay from the input to both the inverting and noninverting outputs of the gate to be approximately the same—18·5 ns $\pm$ 15%. Since the ldomino gate is basically equivalent to two interconnected domino gates (see Fig. 1), its speed and power performance are similar to standard domino gates. In a typical application, such as the design of a 4 bit CMOS ALU, use of the ldomino in the first stage of the logic gates resulted in a 25% saving in layout area, as compared to implementation using standard domino only.

A new technique to enhance the flexibility of domino CMOS circuits has been presented. The ldomino technique can be combined with standard domino or DCVSL gates to implement logic functions, and results in a reduction in area while maintaining domino CMOS circuit speeds. The technique can also be applied to implement CMOS standard cells.[3]

Acknowledgments: This work was supported in part by the Natural Sciences & Engineering Research Council of Canada. One of the authors, J. A. Pretorius, gratefully acknowledges support of the Council of Scientific & Industrial Research, and the University of Pretoria, South Africa.

J. A. PRETORIUS
A. S. SHUBAT
C. A. T. SALAMA

Department of Electrical Engineering
University of Toronto
Toronto, Canada M5S 1A4

7th February 1985

References

1 KRAMBECK, R. H., LEE, C. M., and LAW, H. S.: 'High speed compact circuits with CMOS', *IEEE J. Solid-State Circuits*, 1982, **17**, pp. 614–619
2 HELLER, L. G., GRIFFIN, W. R., DAVIS, J. W., and THOMA, N. G.: 'Cascode voltage switch logic: A differential CMOS logic family'. Proceedings of IEEE international solid state circuits conference, San Francisco, 1984, pp. 16–17
3 PRETORIUS, J. A., SHUBAT, A. S., and SALAMA, C. A. T.: 'Optimization of domino CMOS and its applications to standard cells'. Proceedings of IEEE custom integrated circuits conference, Rochester, NY, USA, 1984, pp. 150–153

INFLUENCE OF AMPLITUDE-PHASE COUPLING ON THE INJECTION LOCKING BANDWIDTH OF A SEMICONDUCTOR LASER

Indexing terms: Lasers and laser applications, Semiconductor lasers

The strong amplitude-phase coupling in a semiconductor laser is well known to induce an enhancement linewidth factor $(1 + \alpha^2)$. It is shown that it also produces an enhancement of the injection locking bandwidth proportional to $(1 + \alpha^2)^{1/2}$. The connection with the usual locking bandwidth derived from Adler's equation is pointed out by considering the carrier dependence of the injected cavity resonance frequency.

Coherent and high-rate lightwave communication systems need stable single-frequency laser sources. Distributed feedback, cleaved-coupled cavity, external feedback and injection locking have been investigated with the aim of achieving stable single-frequency operation of the semiconductor laser. Injection locking of a semiconductor laser has been largely considered previously;[1–5] the usual approach is to consider a wave equation such as the Van der Pol equation with suitable modification to account for optical injection. These studies lead to the well known Adler equation[2] and subsequent classical half-locking bandwidth. However, except for optical feedback, i.e. self-injection locking,[6,7] most of these studies do not include the effect of the carrier-induced refractive index change due to the strong amplitude-phase coupling affecting the semiconductor laser. Our purpose in this letter is to derive a generalised locking bandwidth, taking into account this particular important property of the semiconductor laser and to discuss in this case the meaning of the previously derived half-locking bandwidth formula.

Our model consists of the plane-wave and slowly varying envelope approximation of the cavity field:

$$E(z, t) = \text{Re}\,[E_0(t) \exp(j\omega_0 t - k_m z)] \quad (1)$$

where ω_0 is the laser frequency and k_m the wave number of the mth mode, fixed by the cavity boundary conditions. The optical injection effect of a field with complex amplitude E_{io} in a cavity of length L is included by the complex modal index change[1]

$$\Delta n_i = j\,\frac{c}{\omega_0}\,\frac{1}{2L}\,\frac{E_{io}}{E_0} \quad (2)$$

With the above-mentioned assumptions, the use of eqn. 1 in the wave equation leads to the differential equation given in Reference 6:

$$\frac{\partial E_0}{\partial t} = \left\{\frac{1}{2}\left(G - \frac{1}{\tau_P}\right)(1 + j\alpha)\right. + \frac{c}{2Ln_g}\,\frac{E_{io}}{E_0} - j(\omega_0 - \omega_{mo})E_0 \quad (3)$$

where G is the optical gain, τ_P is the photon lifetime, α is the ratio between the carrier-induced change in the refractive modal index n and the modal gain,[9] n_g is the group index, and

$$\omega_{mo} = \frac{c}{n} k_m \tag{4}$$

is the mth resonance frequency of the unperturbed optical cavity. Although most of the following results can be directly derived from eqn. 3, it is more convenient to convert eqn. 3 into generalised rate equations[10] for the total photon number P and the phase ϕ of the lasing field. Using $E_0 = [\sqrt{(P)} \times \exp(j\phi)]$, one obtains

$$\frac{\partial P}{\partial t} = \left[G - \frac{1}{\tau_P} + \frac{c}{n_g L}\left(\frac{P_i}{P}\right)^{1/2} \cos\theta\right] P \tag{5}$$

$$\frac{\partial \phi}{\partial t} = (\omega_{mo} - \omega_0) + \frac{c}{2n_g L}\left(\frac{P_i}{P}\right)^{1/2} \sin\theta + \frac{\alpha}{2}\left(G - \frac{1}{\tau_P}\right) \tag{6}$$

where P_i is the number of injected photons in the cavity and $\theta = \phi_i - \phi$ is the phase difference between the laser and the injected field.

By eliminating θ between eqns. 5 and 6 it is easy to show that a steady-state solution exists only for ω_0 within the modal half-locking bandwidth, defined as

$$|\omega_{mo} - \omega_0|_{max} = (1 + \alpha^2)^{1/2} \frac{c}{2Ln_g}\left(\frac{P_i}{P}\right)^{1/2} \tag{7}$$

It is to be noted that this locking bandwidth is $(1 + \alpha^2)^{1/2}(c/Ln_g)\tau_P$ times larger than those previously derived, without taking into account the amplitude-to-phase coupling and cavity dispersion. A similar relation has been used very recently for interpreting the observed frequency shift of a laser with optical feedback operation.[11] Fig. 1 shows the half-

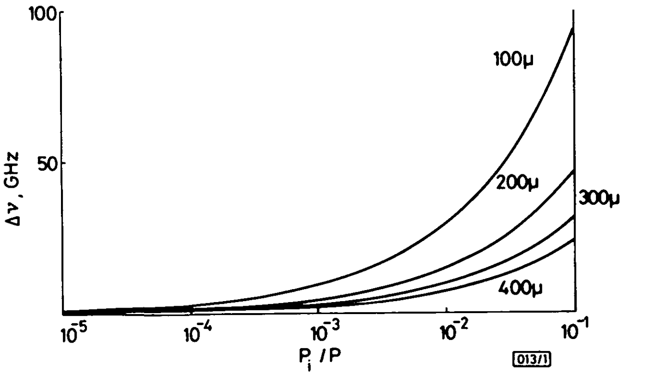

Fig. 1 *Modal half-locking bandwidth against optical injection rate (P_i/P) for various values of cavity length L of a GaAlAs semiconductor laser*

$n_g = 4{\cdot}3$ and $\alpha = 5{\cdot}4$

locking bandwidth given by eqn. 7 against injection ratio P_i/P for various cavity lengths for a GaAlAs semiconductor laser with $n_g = 4{\cdot}3$ and $\alpha = 5{\cdot}4$.

It will now be shown that the usual relation giving the modal half-locking bandwidth, modified to account for dispersion, remains valid but refers to the perturbed cavity resonance frequency.

The carrier-induced change in the refractive index produces a change $\omega_{mi} - \omega_{mo}$, which can be approximated by differentiation of eqn. 4:

$$\omega_{mi} - \omega_{mo} = -\frac{\omega_{mo}}{n_g}\Delta n \tag{8}$$

where Δn is the index change induced by injection, which can be expressed as a function of α and also of $[G - (1/\tau_P)]$, the value of which can be derived from eqn. 5 in the steady-state case:[4]

$$\omega_{mi} - \omega_{mo} = -\alpha \frac{c}{2Ln_g}\left(\frac{P_i}{P}\right)^{1/2} \cos\theta \tag{9}$$

Inserting ω_{mi} from eqn. 9 into eqn. 6 in the steady-state case, one obtains

$$(\omega_{mi} - \omega_0) + \frac{c}{2Ln_g}\left(\frac{P_i}{P}\right)^{1/2} \sin\theta = 0 \tag{10}$$

leading to the well known half-locking bandwidth centred on ω_{mi}:

$$|\omega_{mi} - \omega_0|_{max} = \frac{c}{2Ln_g}\left(\frac{P_i}{P}\right)^{1/2} \tag{11}$$

Fig. 2 shows the relationship between the normalised angular lasing frequency $\bar{\omega}_0 = \omega_0(2Ln_g/c)(P/P_i)^{1/2}$ and θ as expressed

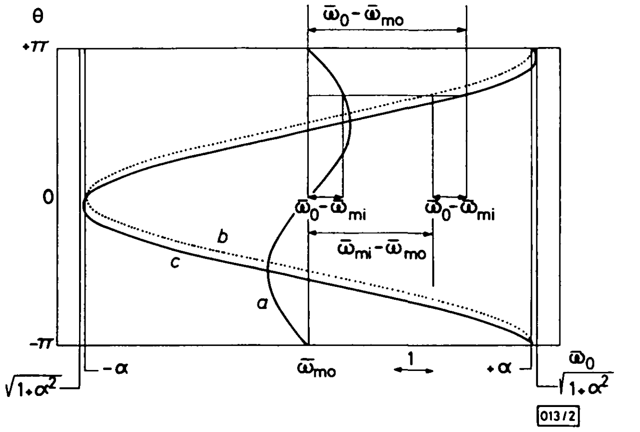

Fig. 2 *Normalised angular lasing frequency $\bar{\omega}_0 = \omega_0(2Ln_g/c)(P/P_i)^{1/2}$ and normalised resonance frequency $\bar{\omega}_{mi}$ of the perturbed cavity as a function of injection phase mismatch θ*

a $\bar{\omega}_0 - \bar{\omega}_{mi}$
b $\bar{\omega}_{mi} - \bar{\omega}_{mo}$
c $\bar{\omega}_0 - \bar{\omega}_{mo}$

by eqns. 9 and 10, and modal half-locking bandwidth as expressed by eqns. 7 and 11. It is to be noted that eqn. 11 is obtained for $\theta = \pm\P$, and that eqn. 7 is obtained for $\tan\theta + (1/\alpha) = 0$, i.e. $\theta = \tan^{-1}(-1/\alpha) + n\P$, where n is an integer. It is clear from this Figure that the mode-locking ceases for these last values of θ and that, as observed by Goldberg *et al.*,[5] the locking bandwidth is no longer symmetrical with respect to ω_{mo}, which is the unlocked lasing frequency.

In conclusion, we have investigated the effect of the carrier-induced index change on the modal half-locking bandwidth of an optical injected laser. We have shown a bandwidth enhancement factor of $(1 + \alpha^2)^{1/2} c\tau_p/Ln_g$ with respect to the usual relation derived from Adler's equation. The latter remains valid, but only when referring to the locking bandwidth calculated from the optically injected cavity resonance frequency. Both explain completely the locking bandwidth asymmetry previously observed.

We gratefully acknowledge Dr. F. Favre for pointing out the importance of dispersion effects.

P. GALLION
G. DEBARGE

12th February 1985

Ecole National Supérieure des Télécommunications
Groupe Optoélectronique et Microondes
Département Electronique et Physique
46 rue Barrault, 75634 Paris Cedex 13, France

References

1 SPENCER, M. B., and LAMB, W. E., JUN.: 'Theory of two coupled lasers', *Phys. Rev. A.*, 1972, 5, pp. 893–898

2 KOBAYASHI, S., and KIMURA, T.: 'Injection locking characteristics of an AlGaAs semiconductor laser', *IEEE J. Quantum Electron.*, 1980, **QE-16**, pp. 915–980
3 LANG, R.: 'Injection locking properties of a semiconductor laser', *ibid.*, 1982, **QE-18**, pp. 976–983
4 FYE, D. M.: 'Relationship between carrier-induced index change and feedback noise in diode lasers', *ibid.*, 1982, **QE-18**, pp. 1675–1678
5 GOLDBERG, L., TAYLOR, H. F., and WELLER, J. F.: 'Locking bandwidth asymmetry in injection-locked GaAlAs lasers', *Electron. Lett.*, 1982, **18**, pp. 986–987
6 AGRAWAL, G. P.: 'Line narrowing in a single-mode injection laser due to external optical feedback', *IEEE J. Quantum Electron.*, 1984, **QE-20**, pp. 468–471
7 SPANO, P., PIAZZOLLA, S., and TAMBURRINI, M.: 'Theory of noise in semiconductor lasers in the presence of optical feedback', *ibid.*, 1984, **QE-20**, pp. 350–357
8 LANG, R., and KABAYASHI, K.: 'External optical feedback effects on semiconductor injection laser properties', *ibid.*, 1980, **QE-16**, pp. 347–355
9 HENRY, C. H.: 'Theory of the linewidth of semiconductor lasers', *ibid.*, 1982, **QE-18**, pp. 259–264
10 AGRAWAL, G. P.: 'Generalized rate equations and modulation characteristics of external cavity semiconductor laser', *J. Appl. Phys.*, 1984, **56**, pp. 3110–3115
11 VODHANEL, R. S., and KO, J. S.: 'Reflection induced frequency shifts in single-mode laser diodes coupled to optical fibres', *Electron. Lett.*, 1984, **20**, pp. 973–974

678 Mbaud OPTICAL TRANSMISSION EXPERIMENT THROUGH 37 km OF PCVD GRADED-INDEX FIBRE

Indexing terms: Optical fibres, Optical transmission

A 5B6B line-coded 565 Mbit/s system designed for single-mode transmission at 1·3 μm wavelength was successfully operated through 37 km of state-of-the-art graded-index fibre (50/125 μm) made by PCVD process. With mean bandwidth values in excess of 1·5 GHz for the individual 2·18 km-long cable sections and a low concatenation factor ($\gamma \simeq 0{\cdot}54$), an overall fibre bandwidth of 400 MHz was achieved. The measured receiver sensitivity was −32·5 dBm for a 10^{-10} BER, showing a penalty of ≤3 dB compared to single-mode transmission.

Up to now the use of graded-index (GI) fibres for long-distance transmission systems (≥20–25 km) has been restricted to transmission speeds up to 140 Mbit/s due to the finite bandwidth-length product of standard fibres from normal production lines. Several of such 140 Mbit/s GI-fibre systems have been installed in West Germany between Hamburg and Hanover with a nominal repeater spacing of 18 km in 1984 (BIGFERN). More systems will go into operation in 1985.

Measurements on the installed BIGFERN cables, containing Philips PCVD fibres showed very good bandwidth and attenuation performance, confirming the high quality of GI fibres produced by the PCVD process.[1,2] These results indicated the possibility to increase either bit rate or repeater section lengths for future GI-fibre systems. In this letter a laboratory transmission experiment at 1·3 μm wavelength with a transmission speed of 678 Mbaud over a distance of 37·06 km is described.

The 2·18 km-long optical cable used in this experiment contained 60 GI fibres (50/125 μm; NA = 0·20) and was taken from normal production. The cable consists of six basic fibre bundles stranded around a central FRP strength member, each bundle comprising ten primary coated fibres in a loose tube. Fig. 1 shows a histogram of the measured attenuation and bandwidth distribution of the individual fibres. 21 of these fibres were welded together by conventional arc-fusion splicing apparatus without power-monitoring to form six groups with section lengths of 2·18, 4·36, 8·72 and 17·44 km, respectively.

The individual groups were terminated with ferruled pigtails, giving the possibility to form concatenated fibre lengths up to 45·8 km in 2·18 km steps by means of standard fibre connectors (F&G 2000 series). The mean splice loss including connectors was 0·16 dB/connection.

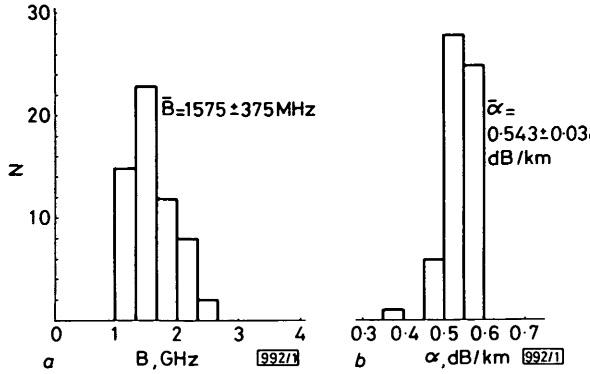

Fig. 1 *Transmission characteristics of the 60 individual fibres*
a Bandwidth distribution relative to 2·18 km
b Attenuation per kilometre

The bandwidths of the individual groups and of several concatenated fibre sections were measured at 1·3 μm by two different test methods, i.e. pulse spreading and swept-frequency technique. 3 dB bandwidths calculated by FFT from the time-domain measurements generally were approximately 10% lower than those obtained from the frequency-domain measurements. This is mainly due to chromatic dispersion effects caused by the larger spectral width of the pulse-modulated laser diode used in the time-domain measurement. ($\Delta\lambda_{FWHM} = 8$ nm compared to $\Delta\lambda_{FWHM} \leq 3$ nm). Nevertheless, both test methods showed Gaussian transfer functions for lengths in excess of 8 km and frequencies up to 1 GHz.

As an example, Fig. 2 shows the frequency characteristic of

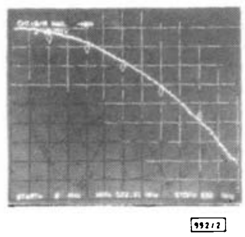

Fig. 2 *Measured frequency response for a 37·06 km-long GI-fibre section, showing a −3 dB frequency of 400 MHz*

Horizontal scale: 50 MHz/div; vertical scale: 1 dB/div (optical)

a 37·06 km-long transmission line. The influence of noise effects on measurement accuracy was extensively reduced by multiple averaging, resulting in a smooth and noise-free curve. The measured bandwidth and attenuation values of several concatenated fibre sections of different lengths are listed in Table 1.

Table 1 BANDWIDTH AND ATTENUATION VALUES FOR CONCATENATED GI-FIBRE LINKS OF DIFFERENT LENGTHS

No.	L, km	BW, MHz	α, dB
1	8·72	920	5·3
2	19·62	640	13·2
3	26·16	495	14·5
4	30·52	460	19·5
5	37·06	400	23·7

Bandwith values corrected for chromatic dispersion effects

The measurements yielded a concatenation factor of $\gamma = 0{\cdot}54$, indicating the high degree of mode mixing present in long lengths of spliced PCVD fibres.[3]

System experiments were carried out with a 5B6B coded 565 Mbit/s system designed for single-mode transmission at 1·3 μm wavelength. Owing to line coding the resulting line transmission speed is 678 Mbaud. The system is described